OCTOBER 15, 2020

LOG INTERPRETATION FOR SOUTH PEPPER – 1.

GEOP4003

PABLO CRESPO CARRILLO
19294973
CURTIN UNIVERSITY

Contents

Introduction

South Pepper – 1 is an abandoned well, drilled in 1982 offshore of Western Australia (Figure 0.1, (GeoscienceAustralia, 2020)). The well discovered hydrocarbons in sandstones from the Barrow Sub-basin (part of the Carnarvon Basin, (GeoscienceAustralia, 2020)).

Figure 0.1 Location of South Pepper - 1

This report is the log interpretation of South Pepper – 1 and cover the following tasks:

1. Quality control of the log data.
2. Calculation of V_{sh} (Volume of shale) from GR.
3. Calculation of sonic porosity (ϕ_S).
4. Calculation of total porosity (ϕ_T) from:
    a. Neutron log.
    b. Density log.
    c. Neutron-Density logs
5. Plot of *Neutron-Density* data on the *Neutron-Density* chart for lithology identification.
6. Calculation of effective porosity (ϕ_e).
    a. From density log.
    b. From neutron log.
    c. From sonic log.
7. Calculation of water resistivity (R_w) from Archie method.
8. Calculation of water saturation (S_w) from Archie method.

1 Quality Control

As part of the quality control, Table 1.1 was generated to summarize the available log information (type, units, and extension).

No.	LOG	UNITS	FROM [m]	TO [m]
1	SP	*MV*	1150	1300
2	CALI	*IN*	1150	1300
3	GR	*API*	1150	1300
4	MSFL	*OHMM*	1150	1300
5	LLS	*OHMM*	1150	1300
6	LLD	*OHMM*	1150	1300
7	DRHO	*G/C3*	1150	1300
8	RHOB	*G/C3*	1150	1300
9	NPHI	*%*	1150	1300
10	DT	*US/F*	1150	1300

Table 1.1 Provided logs to perform log interpretation of South Pepper-1.

The main QC corresponded to removal of tool pick-ups, identification of bad-hole zones, removal of out-of-trend values and correction of depth mismatching. Figure 1.1 displays the original logs, where the following features were marked.

- ✓ Tool pick-ups

Highlighted in red, the tool pick-ups (tails at the base of the curves) were removed from the original logs.

- ✓ Bad-hole flag

Analyzing the caliper log, five zones (in yellow) presented caved holes. Also, no visible presence of mud cakes, although the bit size is unknown. From the caved hole zones it was concluded that only the first zone, around 1165 [m], presented enough damage to affect the other log readings, therefore this interval was removed (gray interval in Figure 1.2).

- ✓ Out-of-trend values

Noisy data at the shallower part of the MSFL was removed from the log since it was not due to changes in the formation but rather problems of the tool while measuring.

- ✓ Depth mismatching

An apparent depth mismatching in the sonic log (DT) was identified, better appreciated with the green-dashed lines that highlights major events in the gamma ray log (used as reference datum).

Figure 1.2 is the logs after QC process. Note how *DT-shift* matches the major events of the *GR* (unlike the original *DT* log).

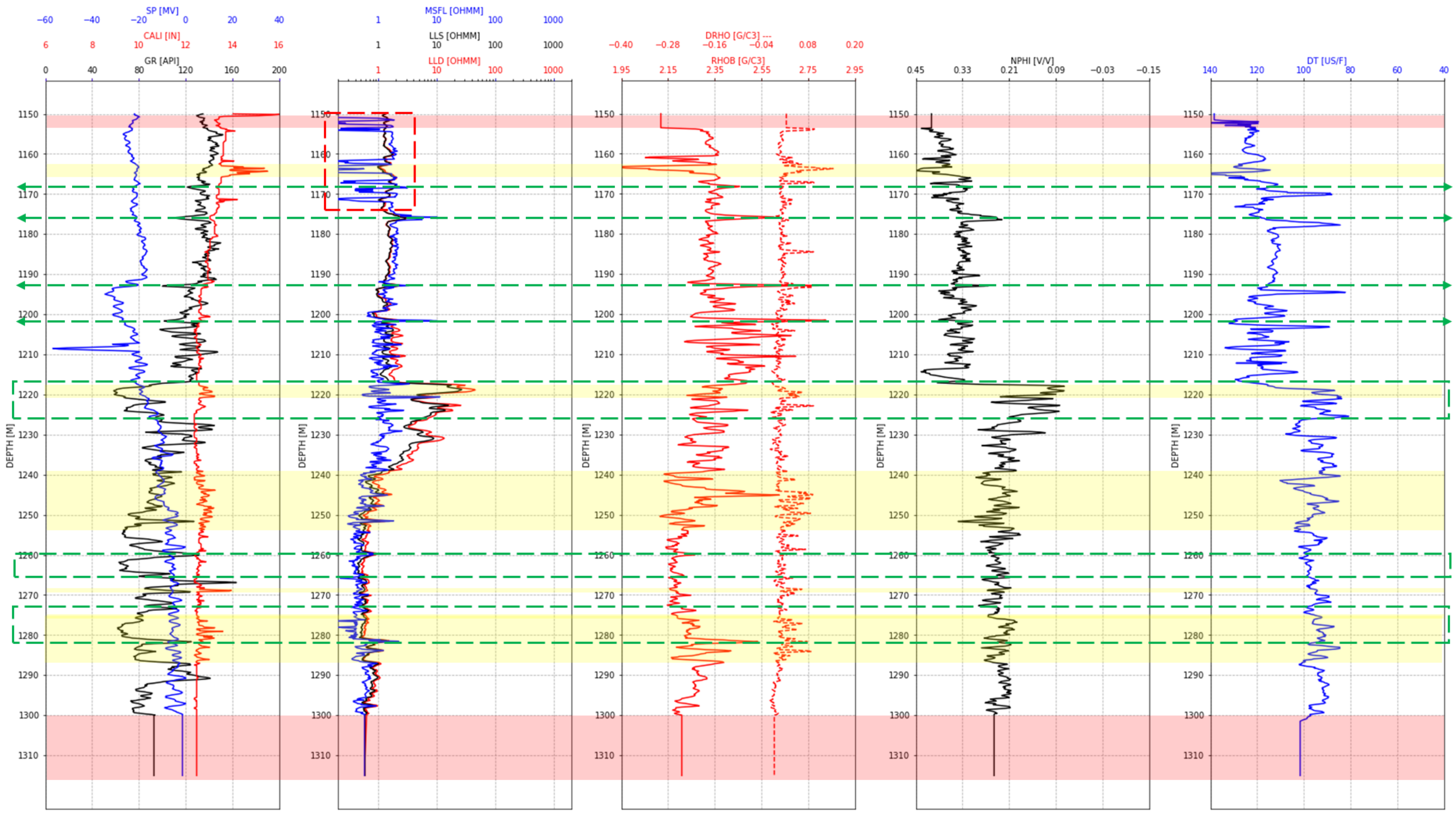

Figure 1.1 Original logs before QC.

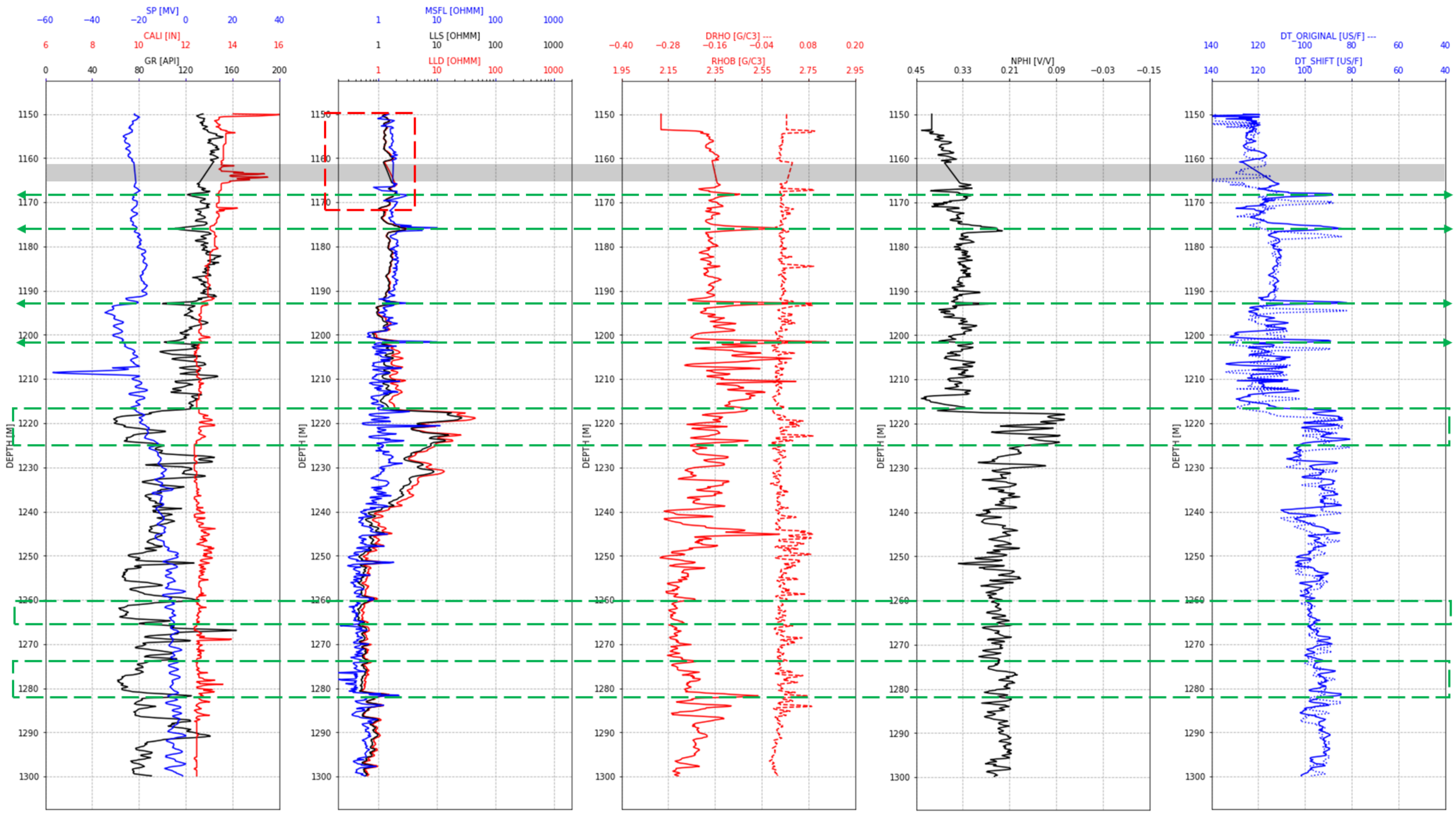

Figure 1.2 Logs after QC.

2 Volume of shale (V_{sh})

Volume of shale was calculated from *GR* assuming a linear relationship and using the *GR index equation*:

$$V_{sh} = \frac{GR_{log} - GR_{min}}{GR_{max} - GR_{min}}$$

As shown in Figure 2.1-left, the sand line and shale line were defined at $65[API]$ and $140[API]$, respectively. From the V_{sh} curve and *GR* log it is possible to define the beginning of a shaly sandstone with shale intercalations at approximately *1217 [m]* depth (blue-dashed line).

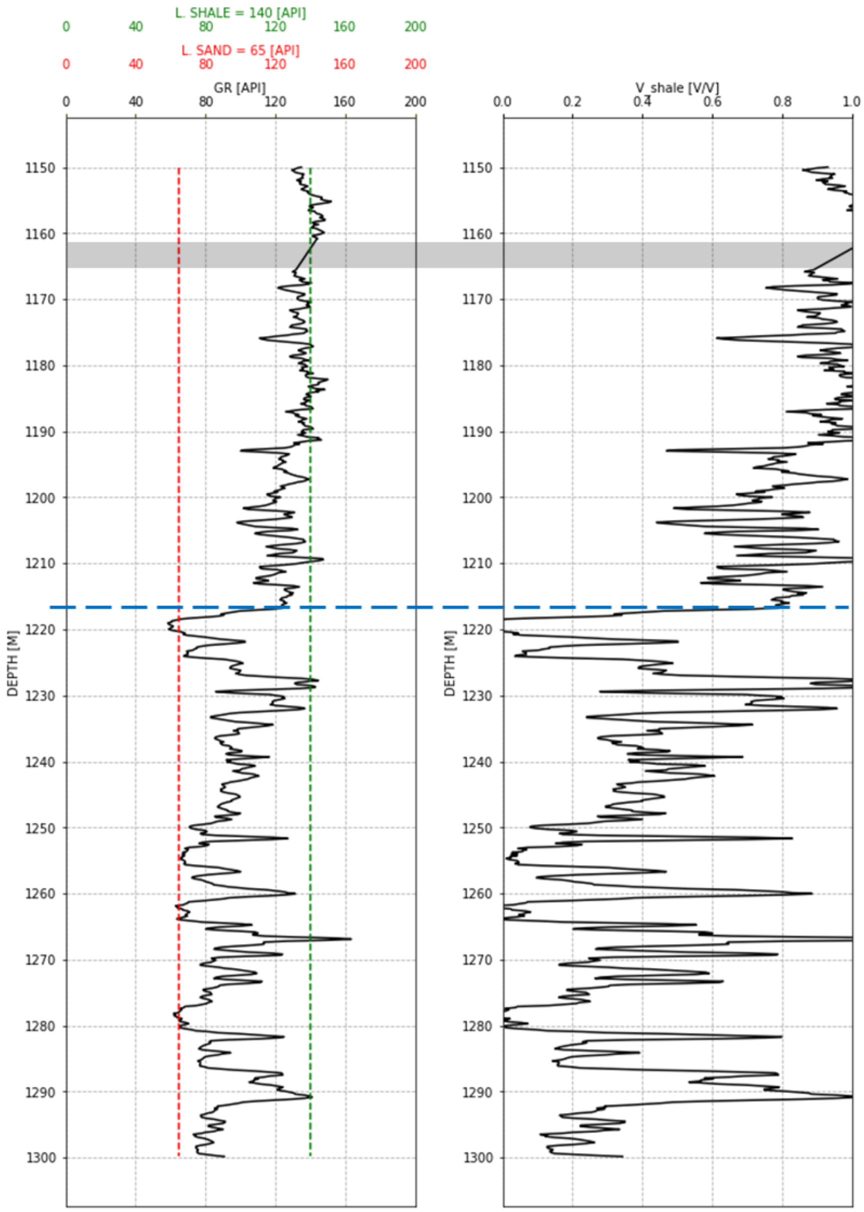

Figure 2.1 GR with sand and shale line and V_{sh}.

3 Sonic Porosity (ϕ_S)

Porosity from sonic log was calculated using the next formula:

$$\phi_S = \frac{DT - DT_{ma}}{DT_f - DT_{ma}}$$

The ϕ_S curve (Figure 3.1) is only valid for the sandstone interval since the transit time of matrix used was quartz. Also, as depths for the target zone are deeper than *1,000 [m]*, salt water was selected for transit time of interstitial fluid:

$$DT_{ma} = DT_{sandstone} = 55.5[\mu s/ft];\ DT_f = DT_{salt\ water} = 185[\mu s/ft]$$

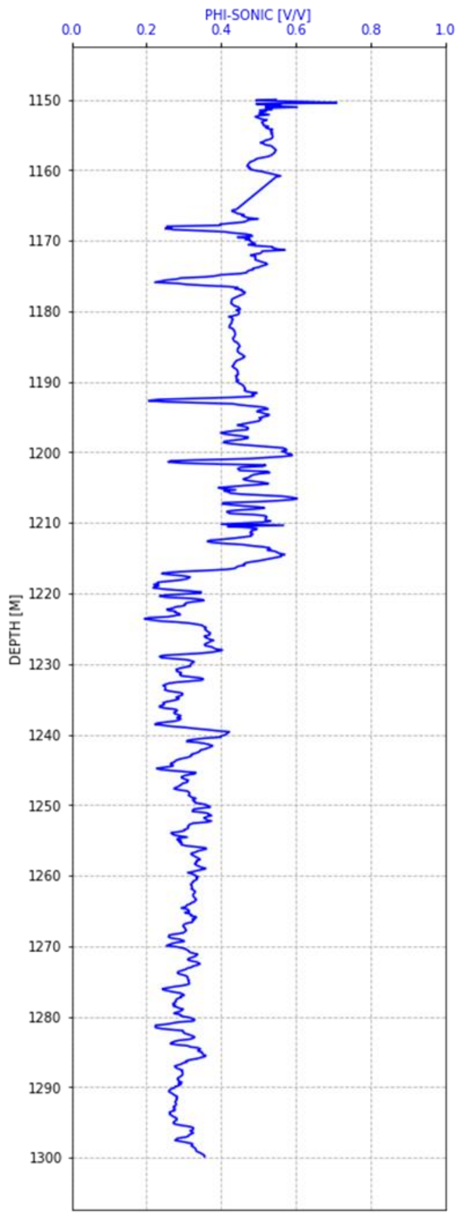

Figure 3.1 Sonic porosity.

4 Total porosity (ϕ_T)

Total porosity was calculated with 3 different methods using Neutron and Density logs, to corroborate that the porosity values are similar.

4.1 From Neutron log

To estimate ϕ_T from the neutron log a matrix correction for sandstones was applied to the neutron log:

$$\phi_T = \phi_N = \phi_{NLOG} - \phi_{MCORR}$$

Where $\phi_{MCORR} = -4$ for sandstones. The total porosity from the neutron log is in Figure 4.1 (black curve).

4.2 From Density log

Total porosity from density log was calculated using the next formula:

$$\phi_T = \phi_D = \frac{\rho_{ma} - \rho_{log}}{\rho_{ma} - \rho_f}$$

Where $\rho_{ma} = 2.65[g/cc]$ is the density of a rock with sandstone matrix and $\rho_f = 1.1[g/cc]$ is the density of saltwater occupying the pore space. The total porosity from the density log is in Figure 4.1 (red curve).

4.3 From Neutron-Density logs

The third method to estimate total porosity was with the Neutron-Density formula for gas bearing formations:

$$\phi_T = \phi_{N-D} = \sqrt{\frac{{\phi_N}^2 + {\phi_D}^2}{2}}$$

A gas bearing formation was selected based on the interpretation presented in Figure 4.2 briefly described below:

Interval	**GR**	**Resistivity logs**	**Neutron-Density logs**	**Shale volume**
Gas zone	Overall good quality shaly sandstone	High resistivity associated to gas presence.	High separation associated to presence of gas.	Interval with at least 50% shale (gray zone).
Oil zone?	Poor quality rock (very shaly sandstone).	Relatively high resistive interval.	Separation of curves less than for gas zone.	High presence of shale.
Transition zone	Low quality rock.	Gradual resistivity increase.	Minor curve separation.	Shaly formation (approx. 50%)
Water zone	Sand formation with shale intercalation.	Low resistivity.	Constant curve separation associated to sandstone.	Presence of high volumes of shale at certain depths.

Total porosity from density log (ϕ_D) was calculated using the formula presented in section 4.2 and ρ_{ma} for limestones equal to 2.71 g/cc and ρ_f for saltwater equal to 1.1 g/cc.

The total porosity from the Neutron-Density formula is in Figure 4.1 (green curve).

Total porosities obtained from the Neutron log, Density log and Neutron-Density log were also plotted in Figure 4.1 to corroborate that the three methods estimate a similar porosity value, which was $\phi_T \approx 30\%$.

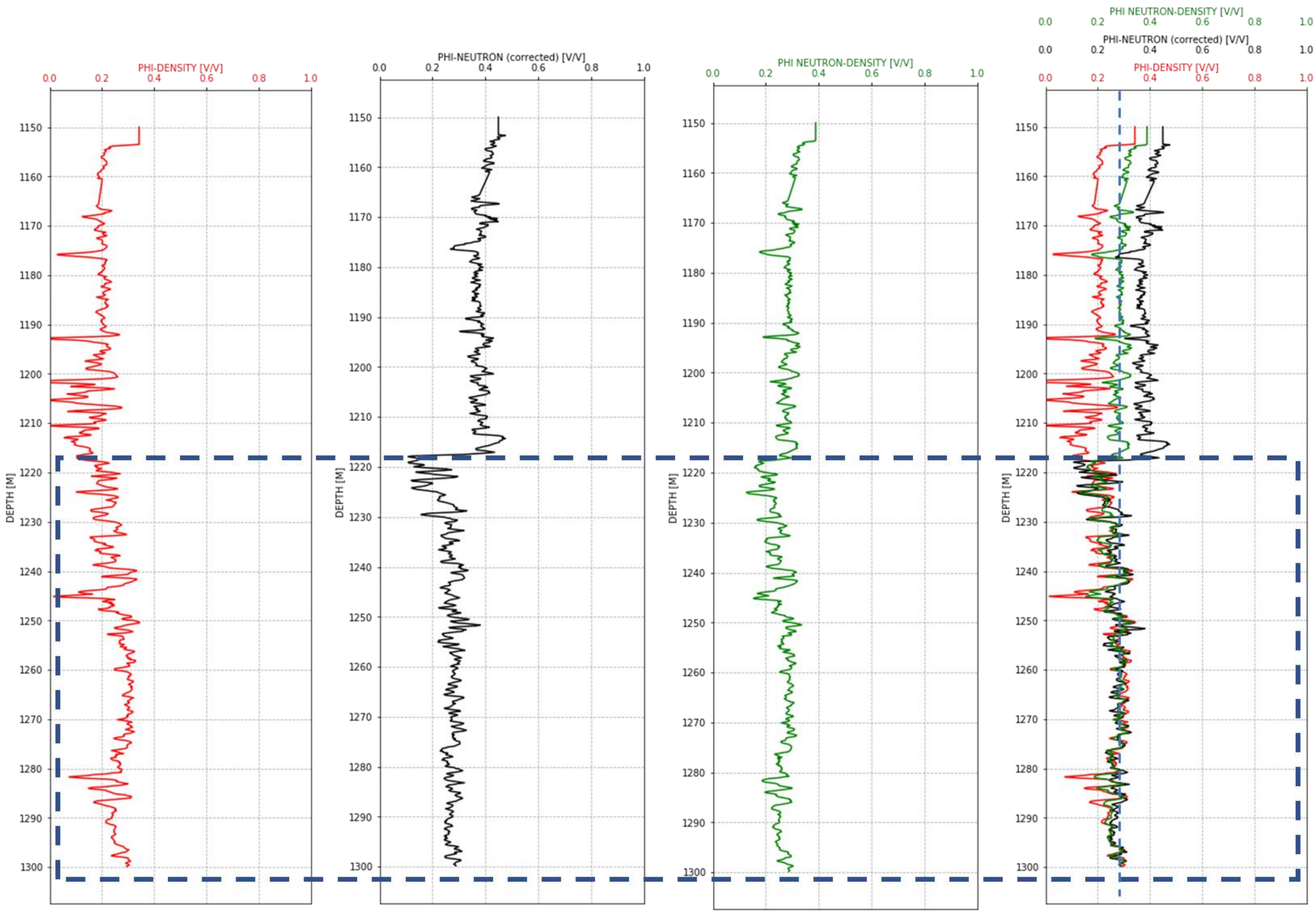

Figure 4.1 Total porosities from density and neutron logs.

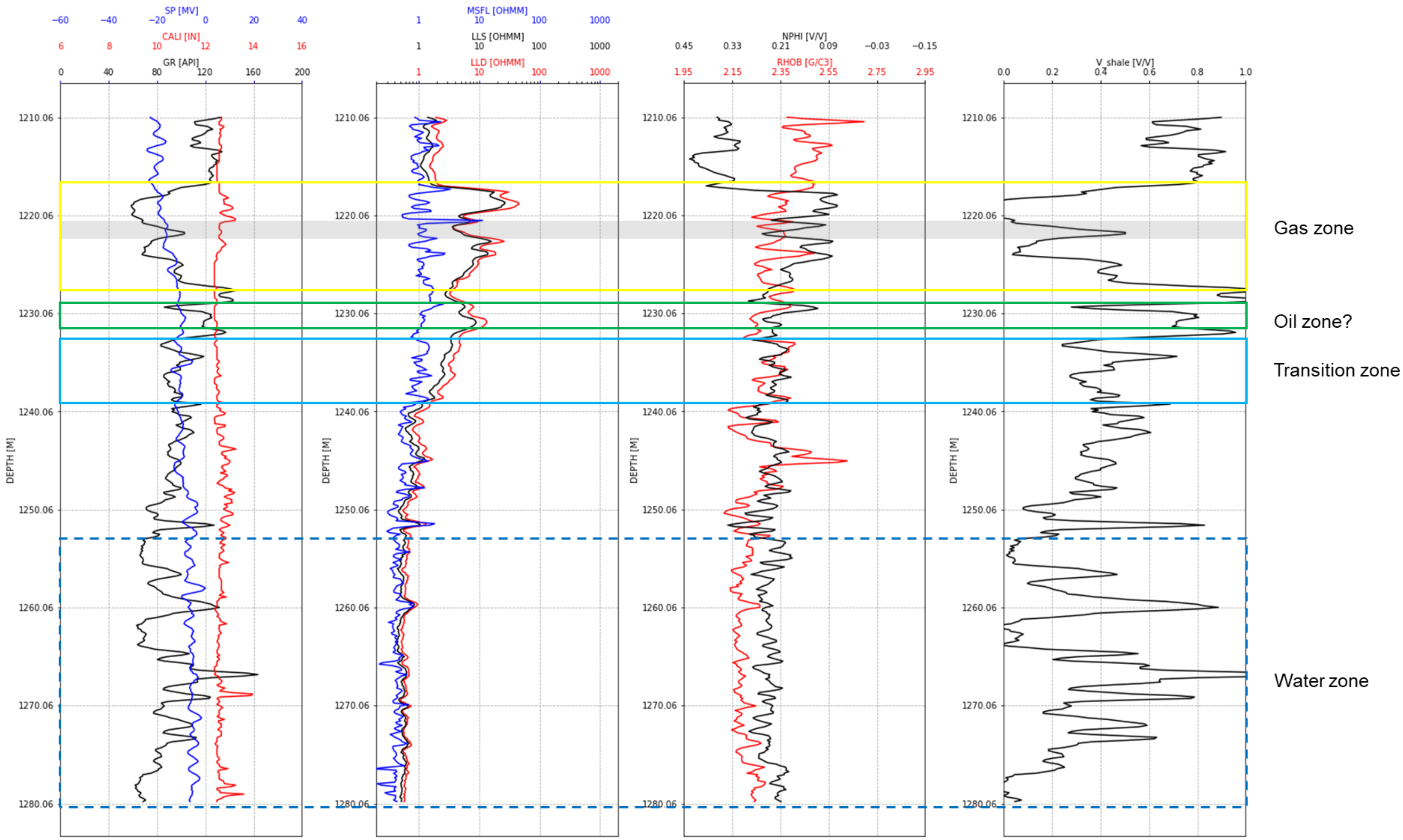

Figure 4.2 Interpretation for the sandstone interval.

5 Neutron-Density chart for lithology identification

The Neutron and Density values for the wet zone were plotted on the Neutron-Density chart for lithology identification.

The data from the wet zone was used to avoid gas effect affecting the Neutron log. However, this zone is affected for shale presence and borehole and mudcake corrections on the Density log as shown in the DRHO curve (Figure 1.2), which may affect the neutron and density readings.

Nevertheless, from Figure 5.1 it is possible to confirm that the reservoir consists mainly of a sandstone with porosity ranging from 25% to 30%, corroborating the total porosity obtained in section 4.

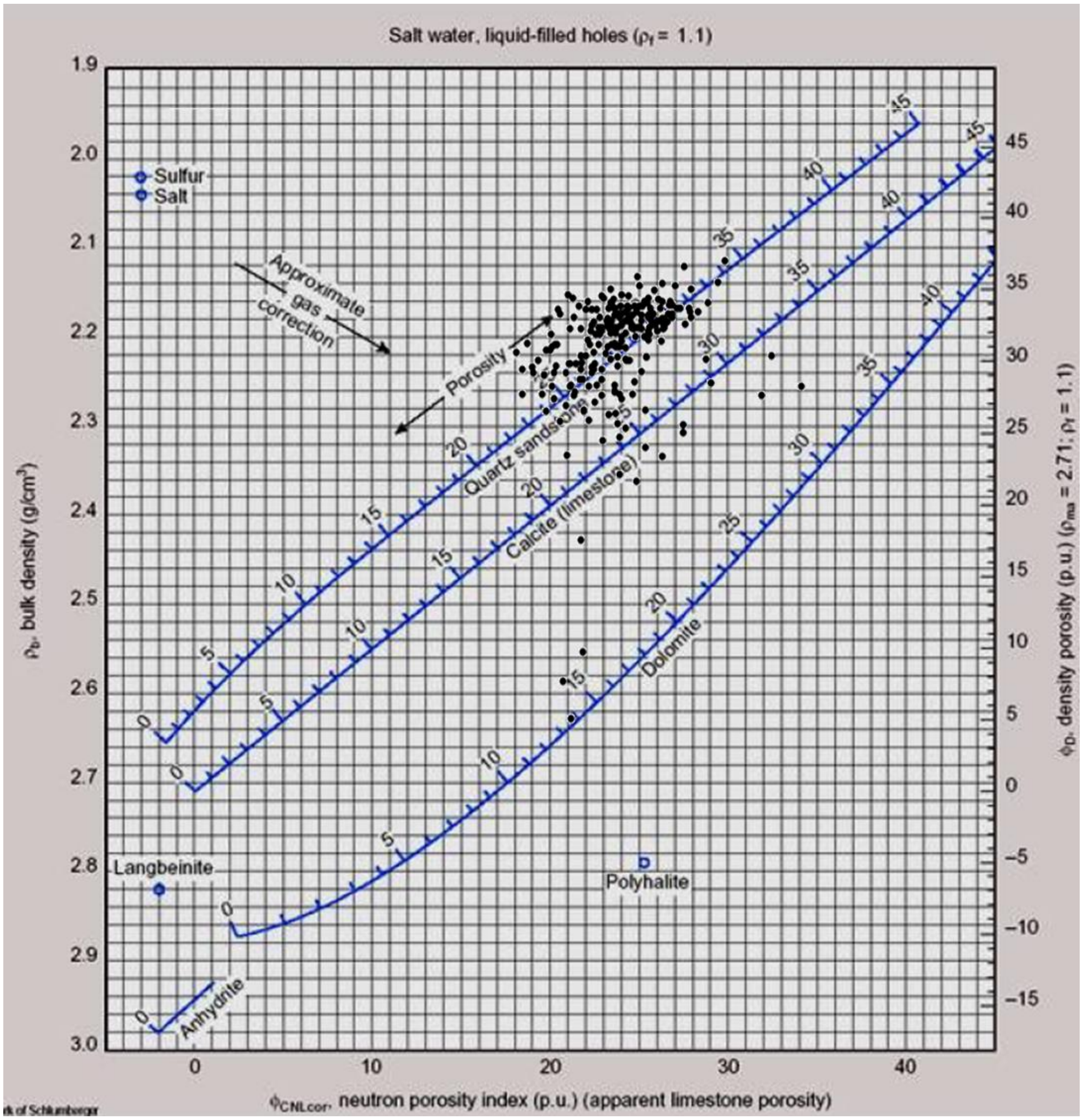

Figure 5.1 Neutron-Density chart for lithology identification.

6 Effective porosity (ϕ_e)

Like total porosity, effective porosity was calculated using three different approaches from density log, neutron log and sonic log.

6.1 From density log

$$\phi_{e_{RHO}} = \frac{\rho_{ma} - \rho_b}{\rho_{ma} - \rho_f} - V_{sh}\frac{\rho_{ma} - \rho_{sh}}{\rho_{ma} - \rho_f}$$

Where ρ_{ma} and ρ_f were defined in section 4.2 and ρ_{sh} was estimated from the thickest close shale interval in the log (green line in Figure 6.1). Effective porosity is presented in Figure 6.1.

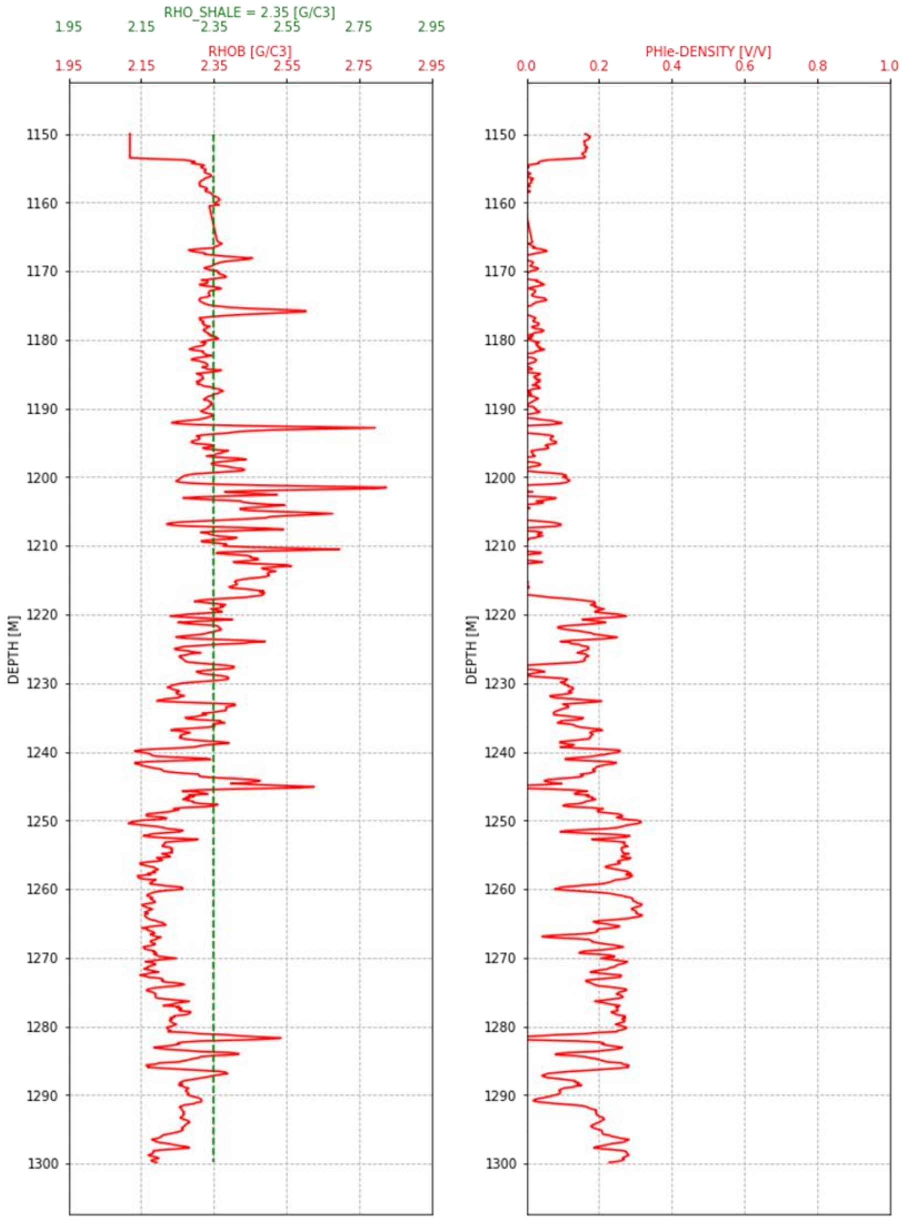

Figure 6.1 Estimated shale value (green line) and effective porosity from density log.

6.2 From neutron log

Like for the density log, neutron value with environment correction associated to shales was defined from the thickest shale interval in the borehole (green line in Figure 6.2). The neutron log in the formula presented below must have environment corrections (calculated in section 4.1).

$$\phi_{eN} = \phi_{Nc} - (V_{sh} \times \phi_{Nc-Sh})$$

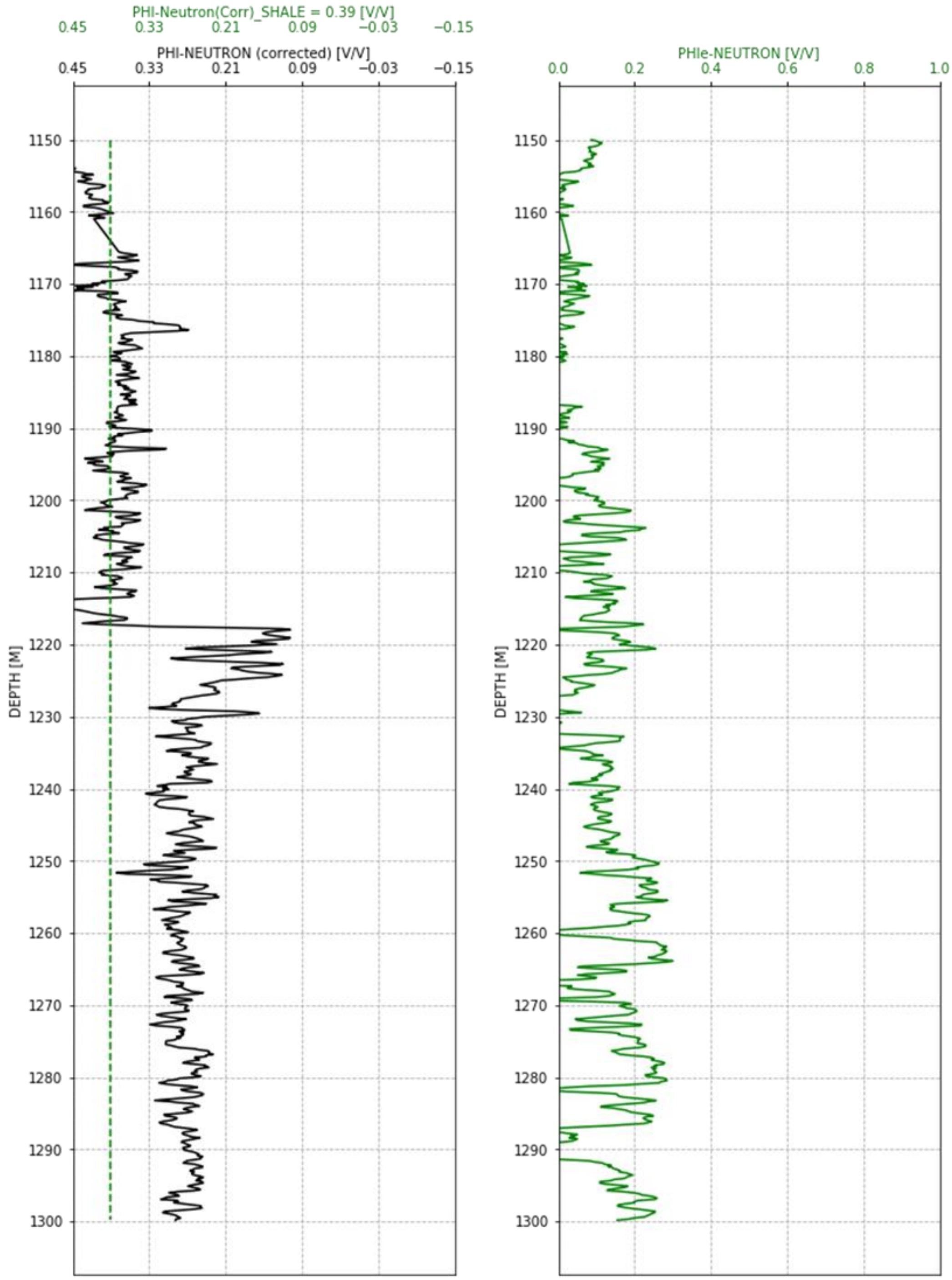

Figure 6.2 Estimated shale value (green line) and effective porosity from neutron log.

6.3 From sonic log

Similar to density log, DT values for the matrix and fluid were defined in section 3, associated to sandstone rock and salt water fluid. DT for shales was estimated from the thickest close shale interval (green line in Figure 6.3). Effective porosity from sonic log is also presented in Figure 6.3.

$$\phi_{eSonic} = \frac{DT_{ma} - DT}{DT_{ma} - DT_f} - V_{sh}\frac{DT_{ma} - DT_{sh}}{DT_{ma} - DT_f}$$

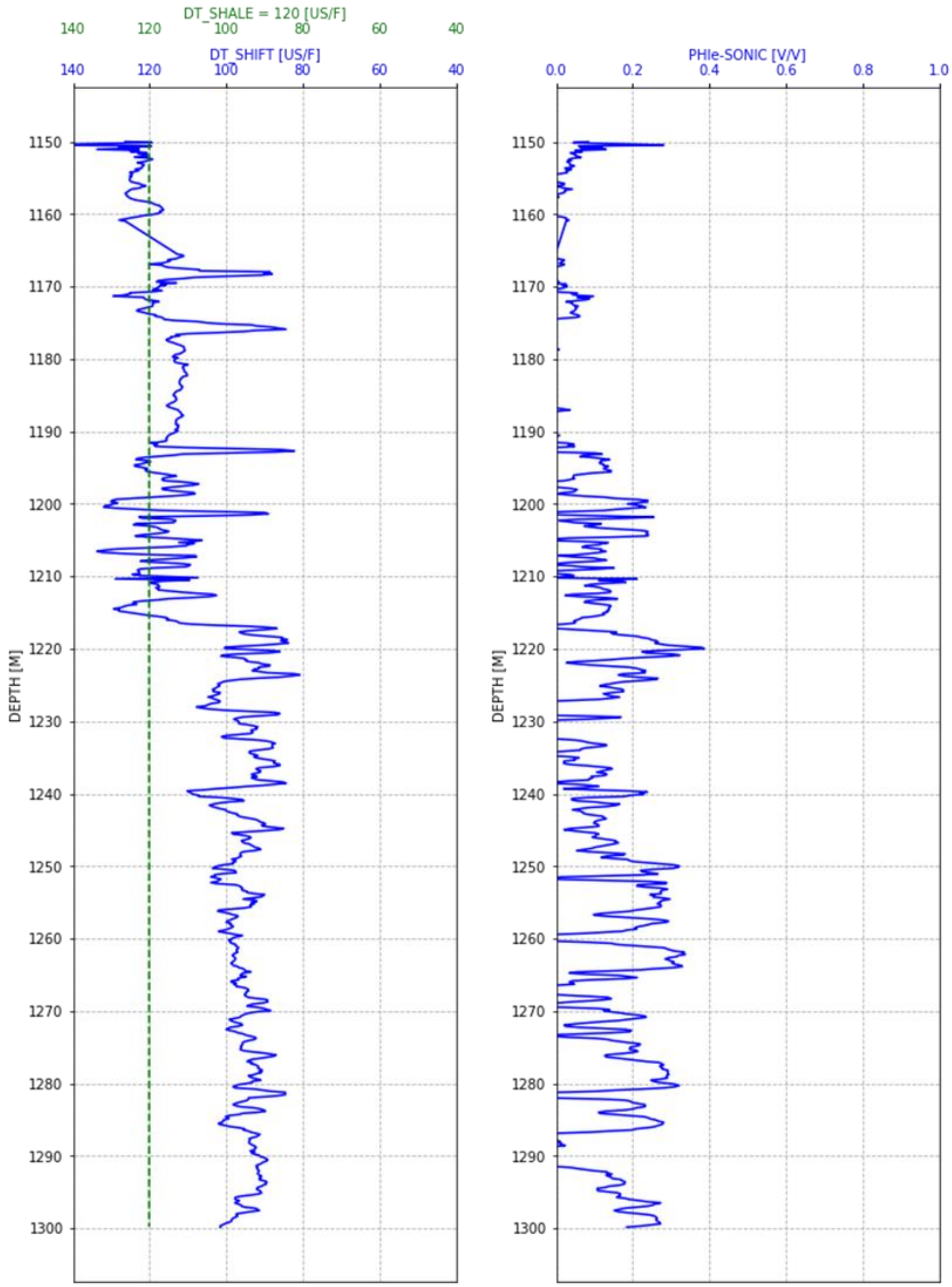

Figure 6.3 Estimated shale value (green line) and effective porosity from sonic log.

A comparison of the three effective porosities is displayed in Figure 6.4 along with resistivity logs. A maximum effective porosity of 30% is observed only at certain intervals, which is an expected output since effective porosity should not be higher than total porosity. Also, the three effective porosities follow the same trend which provides confidence in the results.

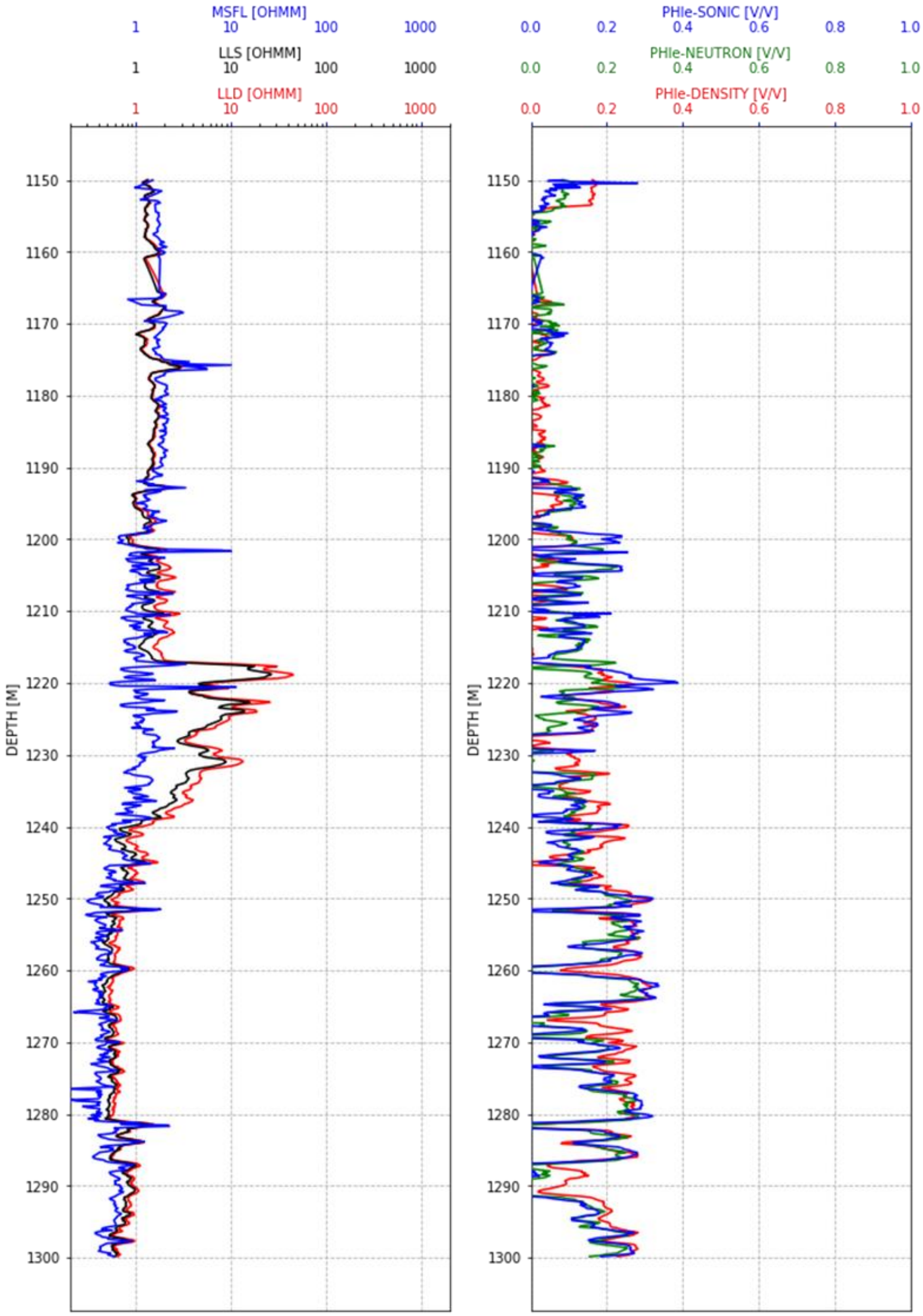

Figure 6.4 Effective porosities from sonic, neutron and density logs.

7 Water Resistivity (R_w)

An apparent water resistivity (R_{wa}) was estimated from the *wet zone* (Figure 7.1) using:

$$R_{wa} = R_t \times \phi^m$$

Where ϕ was obtained from the Neutron-Density log and $R_t = LLD$. The calculated R_{wa} value of 0.05 [OHMM] was assumed to be representative of the whole section (red line in Figure 7.1).

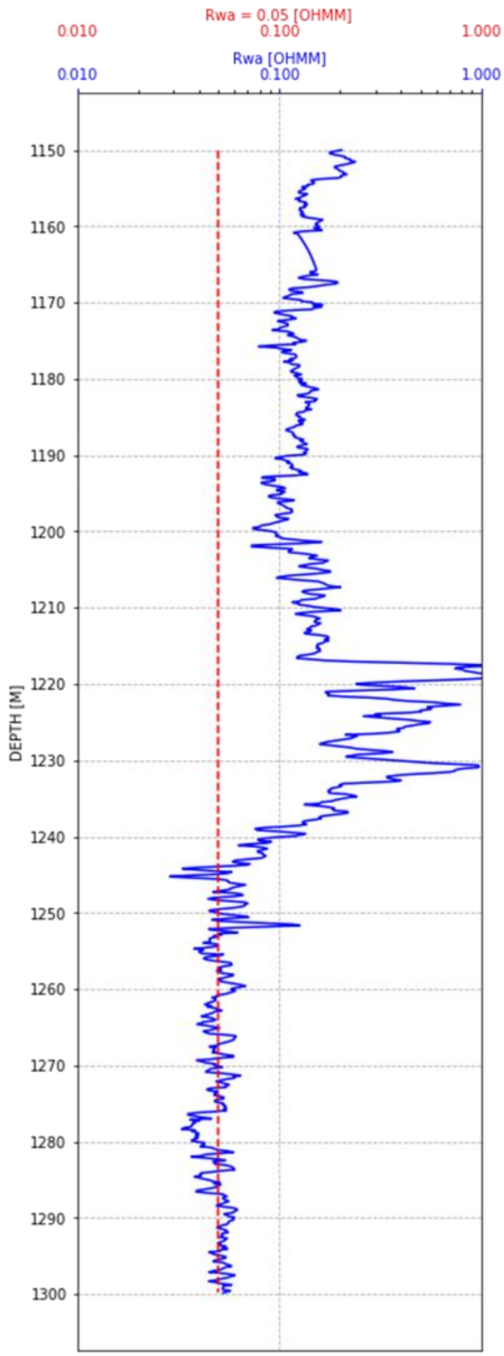

Figure 7.1 Estimated R_{wa} only valid for the reservoir zone.

8 Water Saturation (S_w)

From the apparent water resistivity (R_{wa}) calculated in section 7, the water saturation (S_w, Figure 8.1) was estimated with the next formula:

$$S_w = \sqrt[n]{\frac{a}{\phi^m}\frac{R_{wa}}{R_t}}$$

Where $a = 1$, $m = 2$, $n = 2$, $R_{wa} = 0.05[OHMM]$ and $R_t = LLD$. The zone with hydrocarbon presence has the lowest water saturation (i.e. higher oil saturation, red rectangle in Figure 8.1).

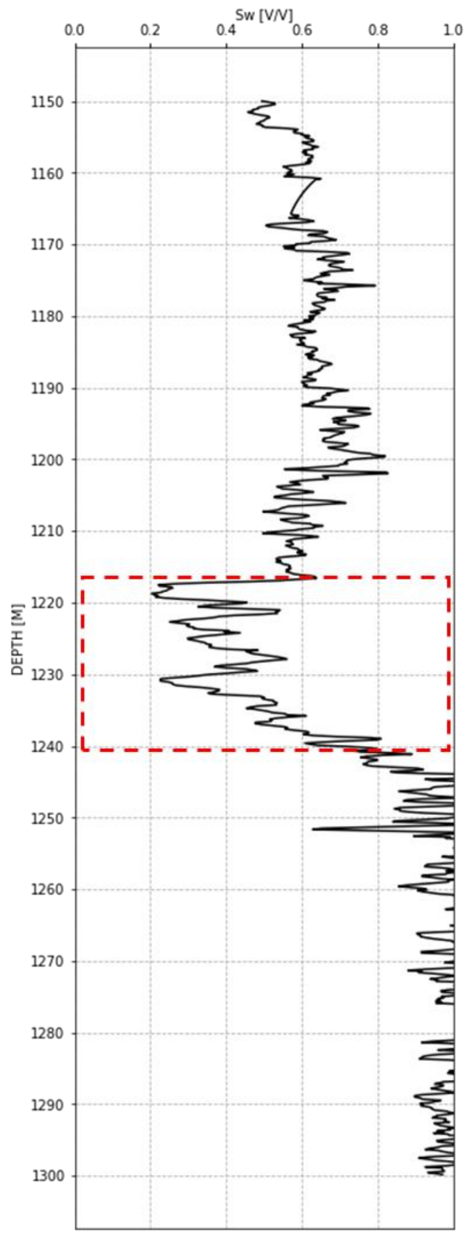

Figure 8.1 Water saturation curve (S_w) with low water saturation at the hydrocarbon zone.

References

1. GeoscienceAustralia, 2020, Carnarvon Basin: http://www.ga.gov.au/scientific-topics/energy/province-sedimentary-basin-geology/petroleum/offshore-northwest-australia/canarvon#heading-2.

2. GeoscienceAustralia, 2020, Well Summary Report, South Pepper 01, http://dbforms.ga.gov.au/www/npm.well.summary_report?pEno=15548&pName=South%20Pepper%2001&pTimescale=A&pTotalDepth=63.107842227378190255220417633410672854&pDepthMax=63.107842227378190255220417633410672854&pDepthMin=0&pPeriod=&pStage=&pAgeMax=1.78&pAgeMin=0&pAgeTop=0&pAgeBase=143.8&pTotalAge=143.8&pPrinterV=Yes, accessed 15-Oct-20.